International Journal of Innovative
Computing, Information and Control
Volume **9**, Number **8**, August **2013**

ICIC International ©2013 ISSN 1349-4198
pp. **3449–3462**

A NEW SECOND-ORDER STRAPDOWN ATTITUDE ALGORITHM

Lei Huang[1,2], Jianye Liu[1], Qinghua Zeng[1] and Zhi Xiong[1]

[1]Navigation Research Center
Nanjing University of Aeronautics and Astronautics
No. 29, Yudao Street, Nanjing 210016, P. R. China
{ huanglei; ljyac; zengqh; xznuaa }@nuaa.edu.cn

[2]Automation Department
Nanjing Forestry University
No. 159, Longpandong Road, Nanjing 210016, P. R. China

Received August 2012; revised December 2012

Abstract. *Typically coning motion has been used as a standard input to assess the performance of the strapdown attitude algorithms. Traditional coning algorithms are based on the Bortz's first-order rotation vector equation. The algorithm error is composed of two parts: drift error and approximation error. For the three (or more)-sample coning algorithms, calculation indicates that approximation error is far larger than drift error for the most general case, which means the approximation error should be reduced firstly. The existing coning algorithms generally increase the sample numbers to reduce drift error, but the increment of the sample numbers has little positive effect on reducing approximation error. To improve the algorithm performance, a new coning algorithm with an additional second-order coning correction term has been developed, which can effectively reduce the approximation error without increasing sample numbers. Simulations and practical tests demonstrate that the new algorithm is superior to the traditional coning algorithms for the general case. Although the new algorithm has increased a little computational load, practical test results validate that with the rapid development of the computer speed, the new second-order strapdown attitude algorithm still satisfies the real-time requirement.*
Keywords: Inertial navigation, Coning algorithm, Approximation error, Drift error

Nomenclature.

α = coning half-angle
Ω = frequency associated with the angular oscillations
ω = angular rate expressed with coordinates in the body frame
$\omega_{A_1A_2}$ = angular rate of coordinate frame A_2 relative to coordinate frame A_1
$\otimes$ = quaternion "multiplication" operator

1. **Introduction.** In strapdown inertial navigation systems, the rotation of an aircraft is measured and integrated to form an attitude matrix which describes the attitude (head, roll and pitch angles) of the body with respect to navigation coordinate frame. However, from the theory of finite rotations [1] we know that when the axis of rotation changes directions, the attitude cannot be determined by direct integration of the body angular rate ω because the direct integration will cause a noncommutativity error. In this case the attitude of a body not only depends on the magnitude, but also depends on the order of the rotations performed [2]. To eliminate the noncommutativity error, rotation vector concept is presented by which we can accurately describe the rotation of a body. The

rotation vector differential equation is [3]:

$$\dot{\Phi} = \omega + \frac{1}{2}\Phi \times \omega + \frac{1}{12}\Phi \times (\Phi \times \omega) \tag{1}$$

The first-order solution to Equation (1) is:

$$\Phi = \int \omega dt + \frac{1}{2}\int (\Phi \times \omega) dt \tag{2}$$

The first term of Equation (2) represents the integration of body angular rate vector. The second term represents the noncommutativity correction by the rotation vector. However, the practical rotation vector algorithms derived from Equation (2) can take various forms.

A classical coning motion is described by quaternion:

$$Q(t) = \left[\cos\frac{\alpha}{2},\ 0,\ \sin\frac{\alpha}{2}\cos\Omega t,\ \sin\frac{\alpha}{2}\sin\Omega t\right] \tag{3}$$

When aircraft is in a coning environment described by Equation (3), the body angular rate ω is:

$$[\omega]^b = 2Q^{-1}(t) \otimes \dot{Q}(t) = \begin{bmatrix} -2\Omega\sin^2\frac{\alpha}{2} \\ -\Omega\sin\alpha\sin\Omega t \\ \Omega\sin\alpha\cos\Omega t \end{bmatrix} \tag{4}$$

where "$[\,]^b$" signifies body axes coordinates. Coning motion described by Equations (3) and (4) can be generated by arbitrary spacecraft maneuvers and spacecraft jitter [4]. [5] proved that when the aircraft is in a coning environment, the noncommutativity correction term of Equation (2) is a maximum. Hence, coning motion is usually used as a particular input to evaluate the attitude integration algorithms of strapdown inertial navigation systems. "Coning motion is also a nonnegligible effect for fast, highly maneuverable precision-pointing spacecraft and alignment calibration for maneuvering spacecraft because state propagation errors can bias the calibration estimates" [4, 6, 7]. In 1996, Ignagni has proved that attitude algorithms work satisfactorily in coning environment will satisfy most other (environments) requirements [8]. Hence, many researches are employed to achieve better performance in a coning environment. In 1983 Miller proposed the traditional three-sample coning algorithm [9]. Based on Miller's algorithm, other improved coning algorithms such as four-sample coning algorithm [10], enhanced algorithm of Miller's three-sample algorithm [11], N-sample general coning algorithm [12], were proposed to satisfy the requirement of high-precision navigation systems. However, all these coning algorithms also have algorithm errors which are composed of two parts: drift error and approximation error. The drift error is caused by the residual constant error on coning axis (x) in the rotation vector calculation. *The approximation error is caused by the approximations in the derivation of the coning algorithms. Hence, the approximation error, like the drift error, is a theoretical error which cannot be reduced by the improvement of the navigation computer's calculation accuracy.*

Traditional coning algorithms ([9, 10, 11, 12]) reduced the drift error by increasing the sample numbers per update period. However, the increment of the sample numbers has little positive effect on reducing approximation error. For the first time, approximation error of the traditional three-sample coning algorithm is calculated in this study. The result indicates that, for the three (or more)-sample coning algorithms, approximation error is far larger than drift error generally. That means approximation error is the major error of the traditional three (or more)-sample coning algorithms. High-precision coning algorithms should give priority to compensate the approximation error rather

than drift error. Hence, it is necessary to study the algorithm which can compensate the approximation error effectively to improve the performance of coning algorithm.

2. Error Analysis of Traditional Three-Sample Coning Algorithm.

2.1. Algorithm flow.

In classical coning motion, three samples of an ideal gyro outputs per update period are:

$$\Delta\theta_i = \int_{t+\frac{i-1}{3}h}^{t+\frac{i}{3}h} \omega dt = \begin{bmatrix} -\frac{2}{3}\Omega h \sin^2\frac{\alpha}{2} \\ -2\sin\alpha\sin\left(\frac{\Omega h}{6}\right)\sin\Omega\left(t+\frac{2i-1}{6}h\right) \\ 2\sin\alpha\sin\left(\frac{\Omega h}{6}\right)\cos\Omega\left(t+\frac{2i-1}{6}h\right) \end{bmatrix}, \quad i=1,2,3 \tag{5}$$

The truth value of updating quaternion is:

$$q(h) = \begin{bmatrix} 1-2\sin^2\frac{\alpha}{2}\sin^2\frac{\Omega h}{2} \\ -\sin^2\frac{\alpha}{2}\sin\Omega h \\ -\sin\alpha\sin\left(\frac{\Omega h}{2}\right)\sin\Omega\left(t+\frac{h}{2}\right) \\ \sin\alpha\sin\left(\frac{\Omega h}{2}\right)\cos\Omega\left(t+\frac{h}{2}\right) \end{bmatrix} \tag{6}$$

The estimated updating quaternion $\hat{q}(h)$ due to the rotation vector is:

$$\hat{q}(h) = \begin{bmatrix} \cos(\Phi/2) \\ (\Phi_x/\Phi)\sin(\Phi/2) \\ (\Phi_y/\Phi)\sin(\Phi/2) \\ (\Phi_z/\Phi)\sin(\Phi/2) \end{bmatrix} = \begin{bmatrix} C \\ \Phi_x S \\ \Phi_y S \\ \Phi_z S \end{bmatrix} \tag{7}$$

where Φ is the magnitude of rotation vector: $\Phi = \sqrt{\Phi_x^2+\Phi_y^2+\Phi_z^2}$.

The error quaternion is:

$$\tilde{q}(h) = q(h)\otimes\overset{\wedge}{q^{-1}}(h) = \begin{bmatrix} q_0C - S(-q_1\Phi_x - q_2\Phi_y - q_3\Phi_z) \\ q_1C - S(q_0\Phi_x - q_3\Phi_y + q_2\Phi_z) \\ q_2C - S(q_3\Phi_x + q_0\Phi_y - q_1\Phi_z) \\ q_3C - S(-q_2\Phi_x + q_1\Phi_y + q_0\Phi_z) \end{bmatrix} \tag{8}$$

Considering q_2, q_3, Φ_y, Φ_z are all periodic, Equation (8) shows that $\tilde{q}_2$, $\tilde{q}_3$ are also periodic and they contribute a reciprocating error. $\tilde{q}_1$ includes nonperiodic term: $q_1C - Sq_0\Phi_x$, which can cause error during the quaternion update. When the update period h is very short, some variables of Equation (8) can be approximated as: $C \approx 1$, $S \approx 1/2$, $q_0 \approx 1$. Then $\tilde{q}_1$ can be simplified to the following form [9]:

$$\tilde{q}_1(h) \approx q_1 - 1/2\Phi_x \tag{9}$$

On the basis of the Bortz's first-order rotation vector equation, three-sample coning algorithm is assumed as [9]:

$$\Phi = \Delta\theta_1 + \Delta\theta_2 + \Delta\theta_3 + k_1\Delta\theta_1\times\Delta\theta_3 + k_2\Delta\theta_2\times(\Delta\theta_3 - \Delta\theta_1) \tag{10}$$

Substitute Equations (5), (6), (10) into Equation (9), based on the minimum error criteria, the optimal coefficient k_i are achieved: $k_1 = 9/20$, $k_2 = 27/40$. Then three-sample coning algorithm is:

$$\Phi = \Delta\theta_1 + \Delta\theta_2 + \Delta\theta_3 + 9/20\Delta\theta_1\times\Delta\theta_3 + 27/40\Delta\theta_2\times(\Delta\theta_3 - \Delta\theta_1) \tag{11}$$

In the past, the drift error (per second) of the coning algorithm defined by Equation (11) was thought as [9]:

$$\sin^2(\alpha/2)\cdot(\Omega^7h^7/51030)/h \tag{12}$$

Note that Equation (12) does not contain approximation error. And the complete algorithm error (including both drift error and approximation error) analysis will be given in the following Equation (19).

Other coning algorithms were developed in order to further reduce drift error [10, 11, 12]. For example, four-sample simplified coning algorithm is developed as follows [10]:

$$\Phi = \theta_1 + \theta_2 + \theta_3 + \theta_4 + 54/105(\theta_1 \times \theta_4) + 92/105(\theta_1 \times \theta_3) + 214/105(\theta_1 \times \theta_2) \tag{13}$$

Four-sample simplified coning algorithm has compensated the drift error on the order of $\sin^2(\alpha/2) \cdot O(\Omega h)^7$. The residual drift error is [10]:

$$(\alpha^2 \Omega^9 h^9/82575360)/h \tag{14}$$

2.2. **Error analysis.** As is stated in Section 2.1, there are some approximations (C, S and q_0) in the derivation of the traditional three-sample coning algorithm. *The error caused by these approximations is referred as approximation error. Obviously, it is a theoretical error which cannot be reduced by the improvement of the computer's calculation accuracy.* The approximation error can be neglected in the moderate accuracy applications, but to the higher-precision systems (e.g., four-sample), it should be considered.

To reduce approximation error, higher-order Taylor series is used:

$$\begin{cases} C = \cos(\Phi/2) = 1 - \Phi^2/8 + \ldots \approx 1 - \Phi^2/8 \\ S = \sin\left(\dfrac{\Phi}{2}\right) \Big/ \Phi = \left[\dfrac{\Phi}{2} - \dfrac{1}{3!} \cdot \left(\dfrac{\Phi}{2}\right)^3\right] \Big/ \Phi + \ldots \approx \dfrac{1}{2} - \dfrac{\Phi^2}{48} \\ q_0 = 1 - 2\sin^2\dfrac{\alpha}{2}\sin^2\dfrac{\Omega h}{2} \end{cases} \tag{15}$$

And from Equation (11) we can obtain:

$$\begin{aligned} \Phi &= \sqrt{\Phi_x^2 + \Phi_y^2 + \Phi_z^2} \\ &\approx \sqrt{16\sin^2\frac{\alpha}{2}\sin^2\frac{\Omega h}{2} + \sin^4\frac{\alpha}{2} \cdot [O(\Omega h)^4 + \ldots]} \\ &\approx 4\sin\frac{\alpha}{2}\sin\frac{\Omega h}{2} \end{aligned} \tag{16}$$

Substitute Equation (15) into Equation (8), the quantization error is achieved:

$$\begin{aligned} \tilde{q}_1 &= q_1 C - S(q_0\Phi_x - q_3\Phi_y + q_2\Phi_z) \\ &\approx -\sin^2\frac{\alpha}{2}\sin\Omega h - \frac{1}{2}\Phi_x + \left(\frac{\Phi^2}{8} \cdot \sin^2\frac{\alpha}{2}\sin\Omega h + \frac{1}{48}\Phi^2\Phi_x + \sin^2\frac{\alpha}{2}\sin^2\frac{\Omega h}{2}\Phi_x\right) \end{aligned} \tag{17}$$

Substitute Equation (11) into Equation (17), and neglect '$\sin 6(\alpha/2)$' and higher-order terms:

$$\tilde{q}_1 = \sin^2\frac{\alpha}{2} \cdot \frac{(\Omega h)^7}{102060} + \sin^4\frac{\alpha}{2}\left[\frac{1}{30}(\Omega h)^5 - \frac{29}{7290}(\Omega h)^7 + \frac{2339}{10333575}(\Omega h)^9 \ldots\right] \tag{18}$$

As is known from [9], the error of coning algorithm Φ_ε equals twice of the quantization error. That is:

$$\Phi_\varepsilon = 2\tilde{q}_1 = \underbrace{\left\{\sin^2\tfrac{\alpha}{2} \cdot \tfrac{(\Omega h)^7}{51030}\right\}}_{\text{drift error}} + \underbrace{\left\{\sin^4\tfrac{\alpha}{2}\left[\tfrac{1}{15}(\Omega h)^5 - \tfrac{29}{3645}(\Omega h)^7 + \tfrac{4678}{10333575}(\Omega h)^9 \ldots\right]\right\}}_{\text{truncation error}} \tag{19}$$

As is seen from Equation (19), the error of traditional three-sample coning algorithm includes two terms. The term in the first brace is the drift error (the same to Equation (12)). The term in the second brace is the approximation error. However, almost

all algorithms ([9, 10, 11, 12]) only specialize in drift error compensation without any consideration on approximation error compensation.

With the rapid development of computing elements, such as DSP and FPGA, the update period h is becoming shorter and shorter, and the effect of approximation error is larger than that of drift error for the general case. For example, given $\alpha = 1^\circ$, $\Omega = 2\pi$rad/s, $h = 10$ms, it is obvious that: $\sin^4(\alpha/2)(\Omega h)^5/15 \gg \sin^2(\alpha/2)(\Omega h)^7/51030$. Therefore, high precision coning algorithms should give priority to compensate the approximation error, and the additional approximation error compensation term $\bar{\delta}_{Tx}$ should be added to the basis of traditional three-sample coning algorithm:

$$\bar{\delta}_{Tx} = \sin^4 \frac{\alpha}{2} \left[\frac{1}{15}(\Omega h)^5 - \frac{29}{3645}(\Omega h)^7 + \frac{4678}{10333575}(\Omega h)^9 \dots \right] \tag{20}$$

3. **New Second-Order Three-Sample Coning Algorithm.** The second-order Bortz's rotation vector equation is:

$$\Phi = \Delta\theta + 1/2 \int_{t_{m-1}}^{t_m} \Phi \times \omega dt + 1/12 \int_{t_{m-1}}^{t_m} \Phi \times (\Phi \times \omega) dt \tag{21}$$

From the traditional coning algorithm, we can get:

$$\Phi = \Delta\theta + \delta\Phi, \quad \delta\Phi \approx 1/2 \int_{t_{m-1}}^{t_m} \Delta\theta \times \omega dt \tag{22}$$

Substitute Equation (22) into Equation (21):

$$\begin{aligned} \Phi =& \Delta\theta + \frac{1}{2} \int_{t_{m-1}}^{t_m} (\Delta\theta \times \omega) dt \\ &+ \left(\frac{1}{4} \int_{t_{m-1}}^{t_m} \left(\int_{t_{m-1}}^{t} \Delta\theta \times \omega dt \right) \times w dt + \frac{1}{12} \int_{t_{m-1}}^{t_m} \Delta\theta \times (\Delta\theta \times \omega) dt \right) \\ =& \Delta\theta + \delta\Phi + \delta\delta\Phi \end{aligned} \tag{23}$$

$\delta\Phi$ represents the noncommutativity compensation of traditional first-order coning algorithms, for example which is expressed by Equation (11). $\delta\delta\Phi$ represents the additional noncommutativity compensation of the new algorithm presented in this paper. The corresponding algorithm of $\delta\delta\Phi$ is discussed as follows.

The gyro output is assumed to be as follows [9]:

$$\Delta\theta = a\tau + b\tau^2 + c\tau^3, \quad \tau = t - t_0, \quad \tau \in (0, h) \tag{24}$$

And

$$\begin{cases} ah = \Delta\theta_3 - 7/2\Delta\theta_2 + 11/2\Delta\theta_1 \\ bh^2 = 9/2(-\Delta\theta_3 + 3\Delta\theta_2 - 2\Delta\theta_1) \\ ch^3 = 9/2(\Delta\theta_3 - 2\Delta\theta_2 + \Delta\theta_1) \end{cases} \tag{25}$$

Substitute Equation (24) into the $\delta\delta\Phi$ term of Equation (23):

$$\begin{aligned} \delta\delta\Phi =& -1/60 b \times (a \times b) h^5 - 1/36 c \times (a \times b) h^6 \\ &+ 1/120 a \times (a \times c) h^5 - 1/72 b \times (a \times c) h^6 \\ &- 5/168 c \times (a \times c) h^7 + 1/180 a \times (b \times c) h^6 \\ &- 1/420 b \times (b \times c) h^7 - 1/120 c \times (b \times c) h^8 \end{aligned} \tag{26}$$

Substitute Equation (25) into Equation (26); after simplifications similar to [9, 11, 12], a conclusion can be obtained that the second-order noncommutativity compensation should

consist of the sum of all second-order cross products formed from the incremental angle vectors for the N subminor sensor-data intervals:

$$\delta\delta\Phi = \sum_{i=1}^{N}\sum_{j=1}^{N-1}\sum_{k=j+1}^{N} l_{ijk}\Delta\theta_i \times (\Delta\theta_j \times \Delta\theta_k), \quad N = 3 \tag{27}$$

Substitute Equation (5) into Equation (27):

$$\begin{aligned}[\Delta\theta_i \times (\Delta\theta_j \times \Delta\theta_k)]_x = &-\frac{16}{3}\Omega h \sin^2\left(\frac{\alpha}{2}\right)\sin^2\alpha\sin^2\left(\frac{\Omega h}{6}\right)\\ &\sin\left(\frac{k-j}{6}\Omega h\right)\sin\left(\frac{2i-j-k}{6}\Omega h\right)\end{aligned} \tag{28}$$

Comparing Equation (20) with Equation (28), we can find that the second-order noncommutativity compensation of $\delta\delta\Phi_x$ can rightly compensate the approximation error of traditional three-sample coning algorithm. Considering Equation (28) is only relevant to the value of $|k-j|$ and $|2i-j-k|$, they have three different values all together:

$$\delta\delta\Phi_x = l_1\Delta\theta_1 \times (\Delta\theta_1 \times \Delta\theta_2) + l_2\Delta\theta_3 \times (\Delta\theta_1 \times \Delta\theta_2) + l_3\Delta\theta_1 \times (\Delta\theta_1 \times \Delta\theta_3) \tag{29}$$

Substitute Equation (28) into Equation (29), using Taylor series to expand '(Ωh)' term, while '$\sin^4(\alpha/2)(\Omega h)^9$' and higher terms were neglected:

$$\begin{aligned}\delta\delta\Phi_x \approx \sin^4\frac{\alpha}{2}\Bigg\{&l_1\left[\frac{4}{243}(\Omega h)^5 - \frac{2}{6521}(\Omega h)^7 + \frac{1}{393660}(\Omega h)^9\right] + l_2\left[-\frac{4}{81}(\Omega h)^5 + \frac{2}{729}(\Omega h)^7\right.\\ &\left.- \frac{23}{393660}(\Omega h)^9\right] + l_3\left[\frac{16}{243}(\Omega h)^5 - \frac{20}{6521}(\Omega h)^7 + \frac{2}{32805}(\Omega h)^9\right]\Bigg\}\end{aligned} \tag{30}$$

As already stated, second-order noncommutativity compensation term $\delta\delta\Phi$ should compensate the approximation error of traditional three-sample coning algorithm. That means $\bar{\delta}_{Tx} = \delta\delta\Phi_x$, where $\bar{\delta}_{Tx}$ was defined in Equation (20). Comparing Equation (30) with Equation (20), we can get:

$$\begin{cases}\dfrac{4}{243}l_1 - \dfrac{4}{81}l_2 + \dfrac{16}{243}l_3 = \dfrac{1}{15}\\ -\dfrac{2}{6521}l_1 + \dfrac{2}{729}l_2 - \dfrac{20}{6521}l_3 = -\dfrac{29}{3645}\\ \dfrac{1}{393660}l_1 - \dfrac{23}{393660}l_2 + \dfrac{2}{32805}l_3 = \dfrac{4678}{10333575}\end{cases} \tag{31}$$

The solution of Equation (31) is very complex. For simplicity, a 16-bit approximate solution is accurate enough:

$$l_1 \approx -14153/73, \quad l_2 \approx 13742/75, \quad l_3 \approx 11401/61 \tag{32}$$

Because the algorithm error on Y, Z axes is reciprocating error, the effect caused by different coefficients on Y, Z axes can be neglected [9]. Then the new higher-precision three-sample coning algorithm which has an additional second-order noncommutativity compensation term is:

$$\begin{aligned}\Phi = &\Delta\theta_1 + \Delta\theta_2 + \Delta\theta_3 + 9/20\Delta\theta_1 \times \Delta\theta_3 + 27/40\Delta\theta_2 \times (\Delta\theta_3 - \Delta\theta_1) - 14153/73\Delta\theta_1\\ &\times (\Delta\theta_1 \times \Delta\theta_2) + 13742/75\Delta\theta_3 \times (\Delta\theta_1 \times \Delta\theta_2) + 11401/61\Delta\theta_1 \times (\Delta\theta_1 \times \Delta\theta_3)\end{aligned} \tag{33}$$

The drift error of Equation (33) is the same as traditional algorithm (Equation (12)), but from Equation (31) we can see that approximation error has been reduced greatly to:

$$\Phi_{\varepsilon/tru} = \sin^4(\alpha/2) \cdot O(\Omega h)^{11} \tag{34}$$

The idea of the new algorithm, which uses an additional second-order noncommutativity compensation term to reduce the approximation error, is also applicable to improve other traditional coning algorithms, such as four-sample coning algorithm, N-sample general coning algorithm. For example, the approximation error of the traditional four-sample coning algorithm can be considered as the same order as that of traditional three-sample coning algorithm [9], but its drift error has been reduced greatly over the three-sample algorithm (Equation (14) vs. Equation (12)). Therefore, to further improve the performance, approximation error should be reduced firstly. Also from the Bortz's rotation second-order vector equation, we can get:

$$\begin{aligned}\Phi &= \Delta\theta + \delta\Phi + \delta\delta\Phi \\ &= \Delta\theta + \sum_{i=1}^{4-1}\sum_{j=i+1}^{4} K_{ij}(\Delta\theta_i \times \Delta\theta_j) + \sum_{i=1}^{4}\sum_{j=1}^{4-1}\sum_{k=j+1}^{4} L_{ijk}\Delta\theta_i \times (\Delta\theta_j \times \Delta\theta_k)\end{aligned} \tag{35}$$

where the optimal value of coefficient K_{ij} has been given by the traditional four-sample coning algorithm (Equation (13)). Similar to Equations (15)-(33), the optimal value of coefficient L_{ijk} can be achieved. Substituting the optimal value into Equation (35), the new second-order four-sample coning algorithm will be obtained.

4. **Error Analysis.**

4.1. **Algorithm I: Traditional three-sample coning algorithm (Equation (11)).** Algorithm I is based on the first-order compensation model; the algorithm error (per second) e_1 consists of drift error e_{1d} and approximation error e_{1T}. They have been calculated in Equation (19):

$$e_1 : \begin{cases} e_{1d} = \sin^2\dfrac{\alpha}{2} \cdot \dfrac{\Omega^7 h^7}{51030}\Big/h \\ e_{1T} = \sin^4\dfrac{\alpha}{2}\left[\dfrac{1}{15}(\Omega h)^5 - \dfrac{29}{3645}(\Omega h)^7 + \dfrac{37561}{94478400}(\Omega h)^9 \ldots\right]\Big/h \end{cases} \tag{36}$$

4.2. **Algorithm II: Traditional four-sample coning algorithm (Equation (13)).** Algorithm II is based on the first-order compensation model too. With the increment of sample numbers, the drift error e_{2d} of Algorithm II has been reduced greatly. However, the approximation error e_{2T} remains the same. The values of e_{2d} and e_{2T} are given in Equation (14) and Equation (19).

$$e_2 : \begin{cases} e_{2d} = \dfrac{\alpha^2\Omega^9 h^9}{82575360}\Big/h \\ e_{2T} = \sin^4\dfrac{\alpha}{2}\left[\dfrac{1}{15}(\Omega h)^5 - \dfrac{29}{3645}(\Omega h)^7 + \dfrac{37561}{94478400}(\Omega h)^9 \ldots\right]\Big/h \end{cases} \tag{37}$$

4.3. **Algorithm III: New second-order three-sample coning algorithm (Equation (33)).** Algorithm III is based on the second-order compensation model. The approximation error e_{3T} is given in Equation (34), from which can see that the approximation error e_{3T} has been reduced greatly. However, the Algorithm III's drift error e_{3d}

is unchanged (as same as Algorithm I). Hence, it has better compensation effects than Algorithm I.

$$e_3 : \begin{cases} e_{3d} = \sin^2 \dfrac{\alpha}{2} \cdot \dfrac{\Omega^7 h^7}{51030} \Big/ h \\ e_{3T} \approx \sin^4 \dfrac{\alpha}{2} [O(\Omega h)^{11} + \ldots] \Big/ h \end{cases} \tag{38}$$

As a conclusion of Equations (36)-(38), the error analyses (per second) of three coning algorithms on X-axis are listed in Table 1.

TABLE 1. Error analyses of three coning algorithms (per second)

Algo.	Φ	X-axis algorithm error (rad/s)
I	Equation (11)	$e_1 = \sin^2 \frac{\alpha}{2} \cdot \frac{\Omega^7 h^6}{51030} + \sin^4 \frac{\alpha}{2} \cdot \frac{1}{15} \Omega^5 h^4$
II	Equation (13)	$e_2 = \sin^4 \frac{\alpha}{2} \cdot \frac{1}{15} \Omega^5 h^4 + \frac{\alpha^2 \Omega^9 h^8}{82575360}$
III	Equation (33)	$e_3 = \sin^2 \frac{\alpha}{2} \cdot \frac{\Omega^7 h^6}{51030} + \sin^4 \frac{\alpha}{2} \cdot O(\Omega^{11} h^{10})$

Table 1 shows that $e_3 \ll e_2 < e_1$ usually. Fox example, given $\alpha = 1^\circ$, $\Omega = 2\pi$, $h = 10$ms, then $e_1 = 3.84 \times 10^{-14}$rad/s, $e_2 = 3.79 \times 10^{-14}$rad/s, and $e_3 = 5.77 \times 10^{-16}$rad/s. The error of Algorithm III was reduced by about order of 2 (152 times) comparing with those of Algorithms I and II. It can be seen that the new second-order coning algorithm (III) has distinct advantages over traditional first-order coning algorithms (I and II).

5. **Computer Loading.** To improve computational efficiency, the calculation of new second-order coning algorithm (Equation (33)) can be separated into two parts:

$$\begin{cases} ① \ X_1 = \Delta\theta_1 \times \Delta\theta_3, \quad X_2 = \Delta\theta_1 \times \Delta\theta_2, \quad X_3 = \Delta\theta_2 \times \Delta\theta_3 \\ ② \ \Phi = \Delta\theta_1 + \Delta\theta_2 + \Delta\theta_3 + \dfrac{9}{20} X_1 + \dfrac{27}{40} (X_2 + X_3) \\ \qquad\quad + \Delta\theta_1 \times \left(\dfrac{11401}{61} X_1 - \dfrac{14153}{73} X_2 \right) + \dfrac{13742}{75} (\Delta\theta_3 \times X_2) \end{cases} \tag{39}$$

As can be seen, calculation of the new second-order coning algorithm (Equation (39)) on three-axis requires 45 multiplications and 39 additions, the traditional three-sample coning algorithm (Equation (11)) on three-axis requires 18 multiplications and 21 additions, the simplified four-sample coning algorithm (Equation (13)) requires 27 multiplications and 27 additions. Note that calculation of the rotation vector only accounts for a tiny portion of total navigation computation. To obtain the actual run time, three attitude algorithms (*not including velocity determination and position determination*) based on Algorithms I, II, III are executed by DSP (TI Co., Ltd, TMS320F28335) with the operating frequency of 150MHz. The mean time-consumption of single execution for each attitude algorithm is listed in Table 2.

Table 2 shows that the actual runtime is slightly different with the theoretical runtime (Algorithm I vs. Algorithm II). These is because TMS320F28335 has the special

TABLE 2. Time-consumption of three attitude algorithms

Attitude algorithm	Φ	Time-consumption
Based on Algorithm I	Equation (11)	22.2μs
Based on Algorithm II	Equation (13)	22.2μs
Based on Algorithm III	Equation (39)	24.2μs

multiply-add unit to optimize the multiply-add operation. Therefore, different programs have different optimized effects by the DSP's C compiler (CCS3.3). From Table 2, we can see that the attitude algorithm (*not including velocity determination and position determination*) based on the new second-order coning algorithm has a computer loading approximately 9% greater than that of the traditional attitude algorithms. And as is stated, the accuracy enhancement is about order of 2. Therefore, the new second-order coning algorithm is as same economical as the traditional coning algorithms. Considering the present IMU's output rate is 50-200Hz (5-20ms once output interval) generally, which is much longer than the time-consumption of the new attitude program. A conclusion can be drawn that the new second-order coning algorithm is applicable to attitude determination.

6. **Simulations.** Validation of the new second-order strapdown attitude integration algorithm is achieved in two steps: 1) Digital simulations are used to verify the error analysis of the coning algorithms given in Equations (35)-(37) are correct; 2) a practical turntable test is carried out to verify the advantages of the new second-order strapdown attitude integration algorithm.

6.1. **Verification the correctness of error analysis given in Equations (35)-(37).** For this 60s duration test, a classical coning motion described by Equation (3) is used as a test input to illustrate the advantages of the new second-order strapdown attitude integration algorithm. The ideal gyro outputs in the coning environment are given in Equation (5). Three coning Algorithms I, II, III are defined in Sections 4.1-4.3.

Rotation vectors calculated by Algorithms I, II, III respectively, are compared with the truth value of rotation vector generated by conversion from the attitude quaternion $q(h)$ (Equation (6)). The $q(h)$ to Φ conversion formula is given in [13], Section 3.2.4.5. Suppose that three coning algorithms use the same gyro, they will have different update periods h. Algorithms I and III use a 3 cycle time period of 0.01s, Algorithm II uses a 4 cycle time period of $0.01 * 4/3$s. Table 3 lists the x-axis errors (per second) of three coning algorithms. The unit of the algorithm error mean (per second) is rad/s, the unit of the algorithm error variance is $(\text{rad/s})^2$.

As is seen from Table 3, the comparison results were similar to the analytical predictions given in Equations (35)-(37). For example, when $\alpha = 1^\circ$, $\Omega = 2\pi$, $h = 10$ms, Algorithm III has the higher accuracy of about 150 times than Algorithm I, which is similar to the theoretical analysis in Section 4. However, in Table 3 it seems that Algorithm II has lower accuracy than Algorithms I, III. This is because when three algorithms use the same gyro output rate, the update period ($h = 0.01 * 4/3$s) of Algorithm II will be longer than that of I, III ($h = 0.01$s). And if the update period h of Algorithm II is also set to 0.01s, the

Table 3. Errors comparisons of three coning algorithms

$\alpha = 1^\circ$	Algorithm I Error ($h = 0.01$s)		Algorithm II Error ($h = 0.01 * 4/3$s)		Algorithm III Error ($h = 0.01$s)	
	Mean (e_1)	*Variance* (e_1)	*Mean* (e_2)	*Variance* (e_2)	*Mean* (e_3)	*Variance* (e_3)
$\Omega = 1$	3.86E-18	5.85E-41	1.22E-17	≈ 0	-1.79E-20	5.85E-41
$\Omega = 2\pi$	3.84E-14	6.68E-38	-1.20E-13	2.96E-37	5.78E-16	6.68E-38
$\Omega = 3\pi$	2.97E-13	7.93E-37	9.07E-13	3.19E-36	9.87E-15	7.93E-37
$\Omega = 5\pi$	4.04E-12	1.08E-35	1.16E-11	4.19E-35	3.52E-13	1.08E-35
$\Omega = 10\pi$	1.62E-10	6.68E-34	-3.66E-10	2.72E-33	4.50E-11	6.68E-34

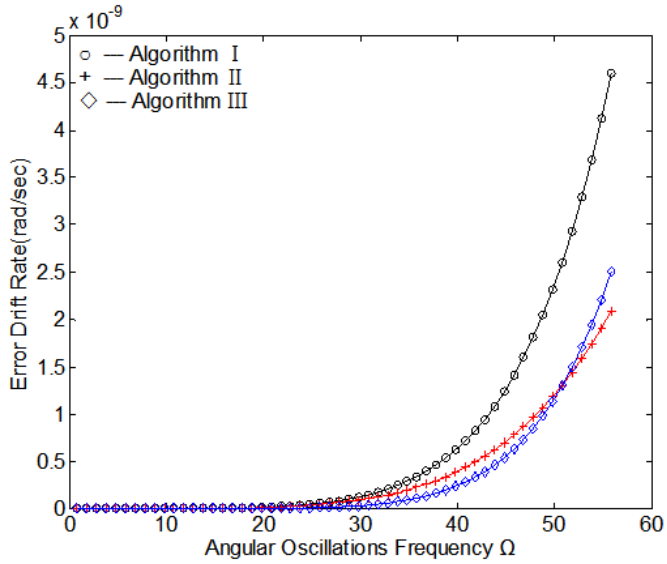

FIGURE 1. Relations between algorithm error and angular oscillations frequency Ω

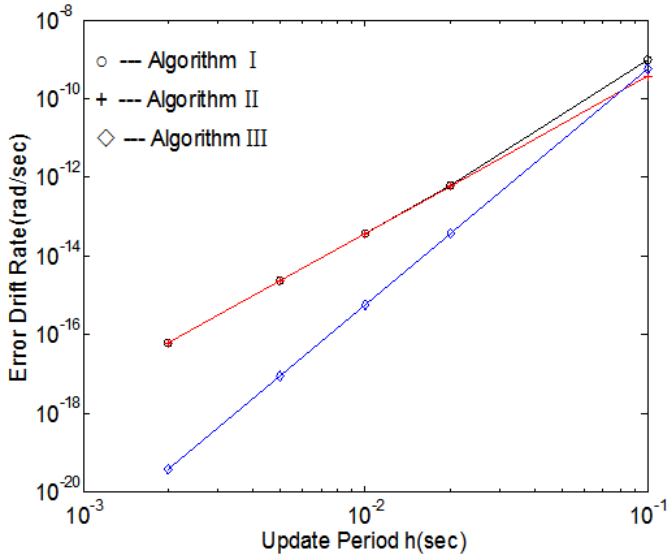

FIGURE 2. Relations between algorithm error and update period h

Algorithm II error will be similar to the analytical predictions of Equation (37). These results provide confidence in the validity of the accuracy analysis for the new algorithm.

Figure 1 shows three coning algorithms errors with different angular oscillations frequency Ω input. For each coning algorithm, the update period h is 10ms and the half-angle coning α is 1°.

From Figure 1, we can see that as the angular oscillations frequency Ω increases, the error of each coning algorithm (I, II, III) increases too. However, on the condition that angular oscillations frequency Ω is the same, the error of the new algorithm is far smaller than that of the traditional three-sample. And when Ω is $0\sim16\pi$, the error of the new algorithm is smaller than that of the traditional four-sample algorithm error too. These results are close to the theoretical predictions given in Equations (35)-(37).

Figure 2 is a log-log plot, which shows the errors (per second) of the three algorithms in different update periods on the condition that the angular oscillations frequency $\Omega = 2\pi$ and half-angle coning $\alpha = 1°$. From Figure 2 we can see that the error of each coning algorithm increases when the update period h becomes longer. However, if the update period h is the same, the error of the new coning algorithm will be far smaller than that of the traditional three-sample coning algorithm (I). And when h is less than about 0.1s, the new algorithm has higher precision than the four-sample coning algorithm (II). The error curve of the new coning algorithm shows a more steep decrease tendency than the error curves of traditional coning Algorithms I, II when the update period h becomes shorter. These results are also close to the theoretical predictions given in Equations (35)-(37).

6.2. **Turntable test to demonstrate the advantages of the new second-order strapdown attitude integration algorithm.** For this 100s duration practical test, a two-axis vibration is produced by a three-axis turntable. The axes of the navigation frame (n) are set to east (x axis), north (y axis), and up (z axis). The used turntable has a work mode of "two-axis vibration" which can simultaneously produce sinusoidal/cosinoidal angular vibrations about the x (pitch channel) and z (head channel) axes. The frequency and amplitude of the vibration about x and z axes are set to 1Hz and 1°. The bias stability of the gyro is 0.01°/hr. The angular rate ω_{nb}^{b} (in body coordinate) caused by vibration are shown in Figure 3, which are achieved by the digital differentiation of the gyro output (angular increment) minus the earth rotation rate projected on body frame. The output rates of the gyro and the turntable are both 50Hz. Hence, the update period h is 0.06s.

From Figure 3 we can see that in such a two-axis vibration environment, the ω_x and ω_z have the same frequency and 90-deg phase shift. So the noncommutativity correction term of Equation (2) will be a maximum on y axis (roll channel). And a cumulative algorithm error will be produced in roll calculation. To illustrate the advantages of the new algorithm, the roll errors caused by using the new second-order attitude integration algorithm and traditional attitude algorithm (based on Algorithm I) are shown in Figures 4 and 5. The truth value of roll is achieved by conversion from the output angle of the turntable (the turntable output is a relative angle to the initial attitude).

Figure 6 is the envelopes of the roll error curves in Figures 4 and 5. From Figure 6 we can see when time is close to 100s, the new attitude algorithm has a smaller roll error about $0.77 * 10^{-3°}$ than the traditional algorithm has. The equivalent decrease of roll error drift is about $2.77 * 10^{-2°}$/hr. This result illustrates that the new algorithm can reduce the coning algorithm error more effectively compared with traditional algorithm.

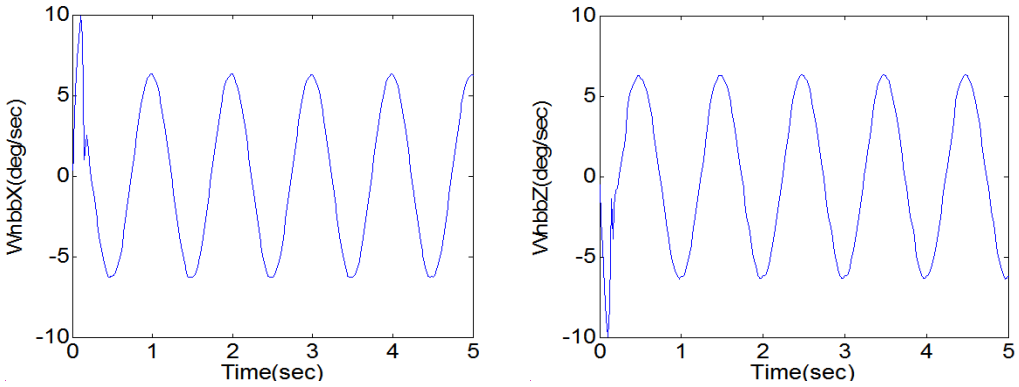

FIGURE 3. Angular rate in body coordinate

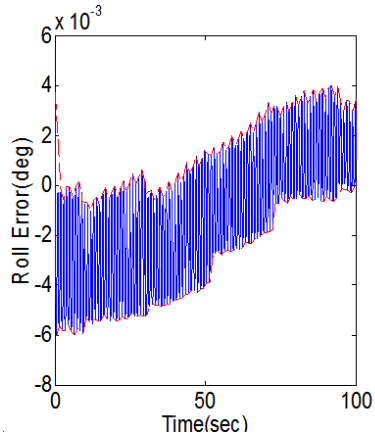

FIGURE 4. Roll error of traditional algorithm

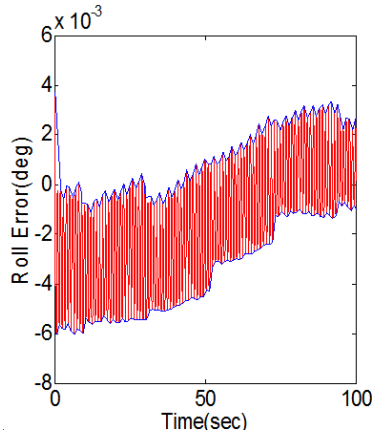

FIGURE 5. Roll error of new algorithm

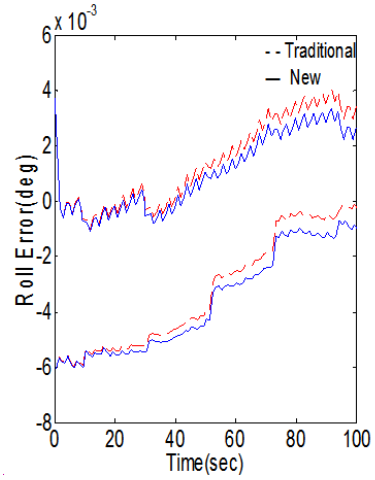

FIGURE 6. A contrast of roll errors drifts

It provides further confidence in the validity of the advantages of the new second-order attitude integration algorithm.

7. **Conclusion.** A second-order strapdown attitude integration algorithm is developed for strapdown inertial navigation systems. The key contributions of the study are:

1) Approximation error of the coning algorithm is first evaluated. The result indicates that for the three (or more)-sample coning algorithms, approximation error is far larger than drift error generally. Hence, approximation error is the major error of the three (or more)-sample coning algorithms. This study presents new approaches for improving the strapdown attitude integration algorithm.

2) A new coning algorithm with an additional second-order coning correction term has been developed. Comparing with the traditional coning algorithms, the new algorithm can effectively reduce the coning algorithm error and sample numbers are not increased. And simulations and practical tests have been presented to illustrate the effectiveness of the developed second-order strapdown attitude integration algorithm.

The new attitude integration algorithm can be applied to strapdown inertial navigation systems, especially for highly dynamic angular motion and high-precision applications. Beyond that, the new second-order attitude integration algorithm can also be applied to highly maneuverable precision-pointing spacecraft and alignment calibration for maneuvering spacecraft because [4, 6, 7] have demonstrated that in these cases coning motion is a nonnegligible effect.

Acknowledgments. This work was supported by the National Natural Science Foundation of China (Grant No. 61104188, 91016019, 61074162, 61174197, 61273057 and 31200496). The authors would also like to acknowledge the assistance of the NUAA Research Funding (No. NS2010084 & NP2011049) & National Basic Research Program of China (No. 2009CB724002), as well as Ji Zhao for his work in the turntable test.

REFERENCES

[1] L. E. Goodman and A. R. Robinson, Effect of finite rotations on gyroscopic sensing devices, *Journal of Applied Mechanics*, vol.25, pp.210-213, 1958.

[2] J. G. Mark and D. A. Tazartes, Tuning of coning algorithms to Gyro data frequency response characteristics, *Journal of Guidance, Control, and Dynamics*, vol.24, no.4, pp.641-647, 2001.

[3] J. E. Bortz, A new mathematical formulation for strapdown inertial navigation, *IEEE Transactions on Aerospace and Electronic Systems*, vol.7, no.1, pp.61-66, 1971.

[4] M. E. Pittelkau, Rotation vector in attitude estimation, *Journal of Guidance, Control, and Dynamics*, vol.26, no.6, pp.855-860, 2003.

[5] H. Musoff and J. H. Murphy, Study of strapdown navigation attitude algorithms, *Journal of Guidance, Control, and Dynamics*, vol.18, no.2, pp.287-290, 1995.

[6] M. E. Pittelkau, Everything is relative in system alignment calibration, *Journal of Spacecraft and Rockets*, vol.39, no.3, pp.460-466, 2002.

[7] M. E. Pittelkau, Kalman filtering for spacecraft system alignment calibration, *Journal of Guidance, Control, and Dynamics*, vol.24, no.6, pp.1187-1195, 2001.

[8] M. B. Ignagni, Efficient class of optimized coning compensation algorithms, *Journal of Guidance, Control, and Dynamics*, vol.19, no.2, pp.424-429, 1996.

[9] R. B. Miller, A new strapdown attitude algorithm, *Journal of Guidance, Control, and Dynamics*, vol.6, no.4, pp.287-291, 1983.

[10] J. G. Lee, J. G. Mark, D. A. Tazartes and Y. J. Yoon, Extension of strapdown attitude algorithm for high-frequency base motion, *Journal of Guidance, Control, and Dynamics*, vol.13, no.4, pp.738-743, 1990.

[11] Y. F. Jiang and Y. P. Lin, Improved strapdown coning algorithms, *IEEE Transactions on Aerospace and Electronic Systems*, vol.28, no.2, pp.486-489, 1992.

[12] G. P. Chan and J. K. Kwang, Formalized approach to obtaining optimal coefficients for coning algorithms, *Journal of Guidance, Control, and Dynamics*, vol.22, no.1, pp.165-168, 1999.

[13] P. G. Savage, *Strapdown Analytics*, Strapdown Associates, Inc., Maple Plain, MN, 2000.

[14] J. Xiong, J. Liu, J. Lai and B. Jiang, A marginalized particle filter in initial alignment for sins, *International Journal of Innovative Computing, Information and Control*, vol.7, no.7(A), pp.3771-3778, 2011.

[15] P. G. Savage, Coning algorithm design by explicit frequency shaping, *Journal of Guidance, Control, and Dynamics*, vol.33, no.4, pp.1123-1132, 2010.